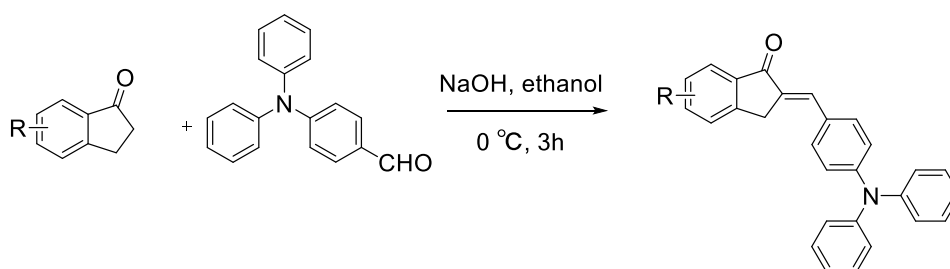


Supporting Information

Microscopic Visualization and Mechanism Investigation on Crystal Jumping Behavior of a Cyclic Chalcone Derivative

*Xiao Cheng, Fulin Yang, Jian Zhao, Juechen Ni, Xinrui He, Chuanjian Zhou, Jing Zhi Sun**,

*Ben Zhong Tang**



Scheme S1. Synthetic procedure of compounds 1–6.

General Information

Materials and Instruments. Chemicals of the highest purity level available were obtained from J&K Scientific, Sigma-Aldrich or Energy Chemical, and were used without further purification. NMR spectra were recorded on a Bruker Avance 400 MHz or Agilent 600 MHz DD2 spectrometer with tetramethylsilane as the internal standard, while mass spectra were recorded on a HP5973GCMS mass spectrometer. Elemental analyses were performed on an Elementar Vario MICRO cube spectrometer. While UV-vis absorption spectra were recorded on a Shimadzu UV-2550 spectrophotometer, emission spectra were recorded using a

Shimadzu RF-5301 PC spectrometer. Absolute fluorescence quantum yields and lifetimes were measured on an Edinburgh FLS920 with or without an integrating sphere.

Synthetic procedure. The synthetic route of compounds **1–6** is shown in Scheme S1.

Aqueous NaOH (1.0 g in 2 ml H₂O) was dropwise added to the mixture of indanone (10 mmol) and 4-(N,N-diphenylamino)benzaldehyde (2.73 g, 10 mmol) in 60 mL ethanol at zero degrees centigrade. The mixture was stirred for 3 h. The precipitates were filtered out, washed with water and cold ethanol, and then dried as crude product. The crude product was recrystallized in CHCl₃/ethanol mixture to give large amount of yellow crystals or crystalline solids. All the crystals of compounds **1–6** were prepared and characterized by NMR. A comparison between the ¹H NMR spectra of **1–4** is shown in Figure S1. The chemical shifts of the hydrogen atoms on the indanone group would be affected by different substituents, while those of the hydrogen atoms on the double bond and the triphenylamine group have little change. Compared with **1**, those hydrogen atoms at 2 and 4 positions in compound **2** obviously show a larger chemical shift, demonstrating that the heavy atom effect of bromo atom would greatly prompt the chemical shift of its neighboring hydrogen to move toward low field. On the other hand, the strong electron-donating effect of bromo atom makes the 1-position hydrogen shows a shift toward high field. The fluorine has little effect on the chemical shifts while the methyl-substituted compound **4** shows a high-field movement at the 2-position. As shown in Figure S2, the location of the bromo atom would largely affect the chemical shifts of the hydrogen atoms on the indanone group. Consequently, compound **5** with bromo at 2-position has a largest chemical shift of 8.02 ppm for the 1-position hydrogen. The synthesis of compounds **7–8** is similar as **1–6** except that the reactant is changed into 6-bromo-1-tetralone in **7** and 4-(N,N-dimethylamino)benzaldehyde in **8**.

(2*E*)-5-bromo-2-[[4-(diphenylamino)phenyl]methylene]-2,3-dihydro-1*H*-inden-1-one (**2**).

Yield: 78%. ¹H NMR (400 MHz, CDCl₃): δ 7.77 (d, *J* = 7.6 Hz, 1H), 7.71 (s, 1H), 7.64 (s, 1H), 7.56 (d, *J* = 7.2 Hz, 1H), 7.51 (d, *J* = 8.8 Hz, 2H), 7.32 (t, *J* = 7.6 Hz, 4H), 7.16 (d, *J* =

7.6 Hz, 4H), 7.13 (t, $J = 7.2$ Hz, 2H), 7.07 (d, $J = 8.4$ Hz, 2H), 4.00 (s, 2H). ^{13}C NMR (100 MHz, CDCl_3): δ 192.9, 150.9, 149.5, 146.6, 137.2, 134.5, 132.1, 131.2, 131.0, 129.5, 129.2, 129.1, 127.8, 125.6, 125.4, 124.3, 121.1, 32.2. MS m/z : 467.15 $[\text{M}]^+$ (calcd: 465.07). Anal. Calcd (%) for $\text{C}_{28}\text{H}_{20}\text{BrNO}$: C, 72.11; H, 4.32; N, 3.00. Found: C, 71.98; H, 4.37; N, 2.85.

(*E*)-5-fluoro-2-[[4-(diphenylamino)phenyl]methylene]-2,3-dihydro-1*H*-inden-1-one (**3**). Yield: 63%. ^1H NMR (400 MHz, CDCl_3): δ 7.83 (d, $J = 8.0$ Hz, 1H), 7.63 (s, 1H), 7.52 (m, 3H), 7.40 (d, $J = 8.4$ Hz, 1H), 7.32 (t, $J = 8.0$ Hz, 4H), 7.16 (d, $J = 7.6$ Hz, 4H), 7.13 (t, $J = 7.6$ Hz, 2H), 7.07 (d, $J = 8.8$ Hz, 2H), 3.98 (s, 2H). ^{13}C NMR (100 MHz, CDCl_3): δ 192.6, 168.0, 165.5, 152.1, 149.5, 146.7, 134.8, 133.9, 132.1, 131.7, 129.6, 128.0, 126.5, 125.6, 124.3, 121.4, 115.7, 112.9, 32.6. ^{19}F NMR (376 MHz, CDCl_3): δ -103.3. MS m/z : 405.25 $[\text{M}]^+$ (calcd: 405.15). Anal. Calcd (%) for $\text{C}_{28}\text{H}_{20}\text{FNO}$: C, 82.94; H, 4.97; N, 3.45. Found: C, 82.66; H, 5.09; N, 3.31.

(*E*)-5-methyl-2-[[4-(diphenylamino)phenyl]methylene]-2,3-dihydro-1*H*-inden-1-one (**4**). Yield: 84%. ^1H NMR (400 MHz, CDCl_3): δ 7.79 (d, $J = 7.6$ Hz, 1H), 7.59 (s, 1H), 7.52 (d, $J = 8.8$ Hz, 2H), 7.31 (m, 5H), 7.22 (d, $J = 8.0$ Hz, 1H), 7.11 (m, 8H), 3.94 (s, 2H), 2.46 (s, 3H). ^{13}C NMR (100 MHz, CDCl_3): δ 194.0, 149.9, 149.2, 146.8, 145.4, 136.1, 133.4, 132.6, 132.0, 129.5, 128.8, 128.5, 126.5, 125.5, 124.1, 121.5, 32.5, 22.2. MS m/z : 401.25 $[\text{M}]^+$ (calcd: 401.18). Anal. Calcd (%) for $\text{C}_{29}\text{H}_{23}\text{NO}$: C, 86.75; H, 5.77; N, 3.49. Found: C, 85.81; H, 5.80; N, 3.31.

(*E*)-6-bromo-2-[[4-(diphenylamino)phenyl]methylene]-2,3-dihydro-1*H*-inden-1-one (**5**). Yield: 69%. ^1H NMR (400 MHz, CDCl_3): δ 8.02 (s, 1H), 7.69 (d, $J = 8.0$ Hz, 1H), 7.63 (s, 1H), 7.51 (d, $J = 8.8$ Hz, 2H), 7.15 (d, $J = 8.0$ Hz, 1H), 7.32 (t, $J = 8.0$ Hz, 4H), 7.16 (d, $J = 8.0$ Hz, 4H), 7.12 (t, $J = 7.2$ Hz, 2H), 7.06 (d, $J = 8.8$ Hz, 2H), 3.93 (s, 2H). ^{13}C NMR (100 MHz, CDCl_3): δ 192.8, 149.6, 147.9, 146.6, 140.3, 136.8, 134.8, 132.2, 131.5, 129.6, 127.8, 127.7, 127.2, 125.7, 124.4, 121.8, 121.2, 32.3. MS m/z : 467.15 $[\text{M}]^+$ (calcd: 465.07). Anal. Calcd (%) for $\text{C}_{28}\text{H}_{20}\text{BrNO}$: C, 72.11; H, 4.32; N, 3.00. Found: C, 71.68; H, 4.32; N, 2.80.

(2*E*)-4-bromo-2-[[4-(diphenylamino)phenyl]methylene]-2,3-dihydro-1*H*-inden-1-one (**6**).

Yield: 60%. ¹H NMR (400 MHz, CDCl₃): δ 7.85 (d, *J* = 7.6 Hz, 1H), 7.75 (d, *J* = 7.6 Hz, 1H), 7.66 (s, 1H), 7.57 (d, *J* = 8.8 Hz, 2H), 7.32 (m, 5H), 7.17 (d, *J* = 7.6 Hz, 4H), 7.13 (t, *J* = 7.2 Hz, 2H), 7.09 (d, *J* = 8.8 Hz, 2H), 3.91 (s, 2H). ¹³C NMR (100 MHz, CDCl₃): δ 193.5, 149.7, 149.3, 146.6, 140.5, 136.8, 135.1, 132.4, 131.0, 129.6, 129.4, 127.7, 125.8, 124.4, 123.0, 121.6, 121.1, 33.8. MS *m/z*: 467.25 [M]⁺ (calcd: 465.07). Anal. Calcd (%) for C₂₈H₂₀BrNO: C, 72.11; H, 4.32; N, 3.00. Found: C, 72.21; H, 4.35; N, 2.83.

5,5"-dibromo-2',4'-bis(4-(diphenylamino)phenyl)dispiro[indene-2,1'-cyclobutane-3',2"-indene]-1,1"(3*H*,3"*H*)-dione (***d*-2**). Yield: 53%. ¹H NMR (600 MHz, CDCl₃): δ 7.61 (s, 2H), 7.50 (d, *J* = 7.8 Hz, 2H), 7.46 (d, *J* = 7.8 Hz, 2H), 7.21 (t, *J* = 7.8 Hz, 8H), 6.99 (m, 12H), 6.86 (s, 8H), 4.51 (s, 2H), 3.71 (d, *J* = 18 Hz, 2H), 3.56 (d, *J* = 18 Hz, 2H). MALDI-TOFMS *m/z*: 933.596 [M]⁺ (calcd: 932.14). Anal. Calcd (%) for C₅₆H₄₀Br₂N₂O₂: C, 72.11; H, 4.32; N, 3.00. Found: C, 72.01; H, 4.35; N, 2.83.

Single-crystal X-ray Diffraction.

Single-crystal X-ray diffraction data were collected on a Oxford (Varian) Gemini A Ultra diffractometer in ω-scan mode using graphite-monochromated Mo-Kα radiation. Structures were solved with direct methods using the SHELXTL program and refined with full-matrix least squares on *F*². Non-hydrogen atoms were refined anisotropically, while the positions of hydrogen atoms were calculated and refined isotropically. [CCDC 1854436 for **1**, 1854435 for **2**, 1854440 for **4**, 1854437 for **5**, 1854442 for **6**, 1854438 for **7**, 1854439 for **8**, 1854441 for ***d*-2** contain the supplementary crystallographic data for this paper. These data can be obtained free of charge from The Cambridge Crystallographic Data Centre via www.ccdc.cam.ac.uk/data_request/cif.]

Calculations.

All the geometries came from the single crystal data, and the calculations were performed by ORCA 4.1.0^[1,2] at RI-B3LYP/def2-TZVP level of theory with fine integration grid for both

B3LYP and RICOSX, containing the atom-pairwise dispersion correction with the Becke-Johnson damping scheme (D3BJ)^[3]. The Multiwfn 3.6 package^[4] was utilized to extract the cube file of the value of orbital wavefunction and reduced density gradient (RDG)^[5] by using the molden file generated from the ORCA calculation. The cube files were regarded as the input file for VMD 1.9.3^[6], for which was used to visualize the graphs of HOMO and LUMO as well as the RDG at the isosurface at 0.01 and 0.50, respectively.

References

- [1] F. Neese, "The ORCA program system" *Wiley Interdisciplinary Reviews: Computational Molecular Science*, 2012, Vol. 2, Issue 1, Pages 73-78.
- [2] F. Neese, "Software update: the ORCA program system, version 4.0" *Wiley Interdisciplinary Reviews: Computational Molecular Science*, 2017, Vol. 8, Issue 1, p. e1327.
- [3] S. Grimme, S. Ehrlich, L. Goerigk. *J. Comp. Chem.* **2011**, 32, 1456.
- [4] T. Lu, F. Chen, *J. Comp. Chem.* **2012**, 33, 580.
- [5] E. R. Johnson, S. Keinan, P. Mori-Sanchez, J. Contreras-Garcia, A. J. Cohen, W. Yang, *J. Am. Chem. Soc.* **2010**, 132, 6498.
- [6] W. Humphrey, A. Dalke, K. Schulten, *Journal of molecular graphics* **1996**, 14, 33.

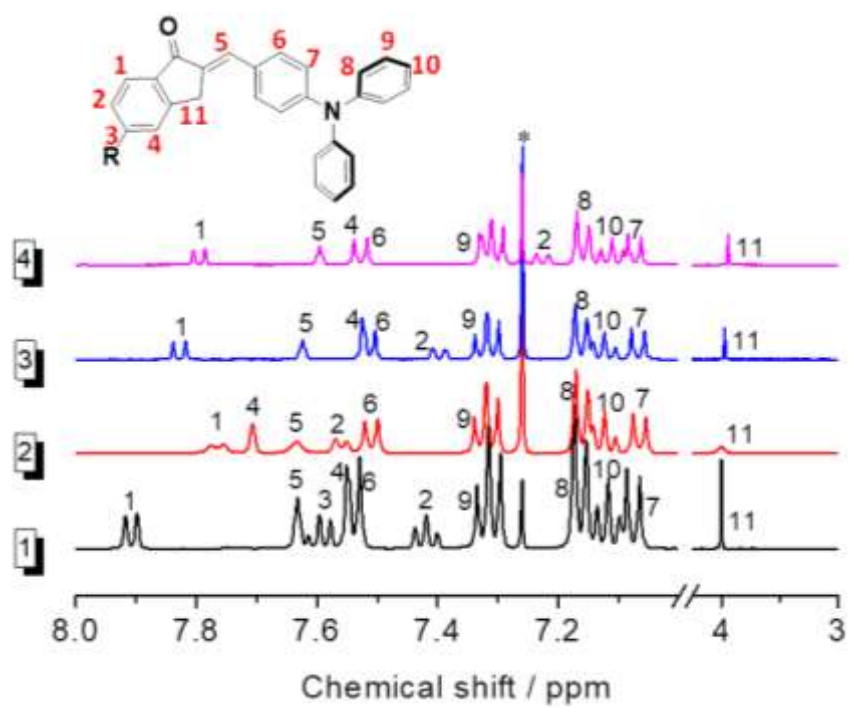


Figure S1. A comparison of the chemical shifts of ^1H NMR spectra for compounds **1–4** in CDCl_3 (500 MHz).

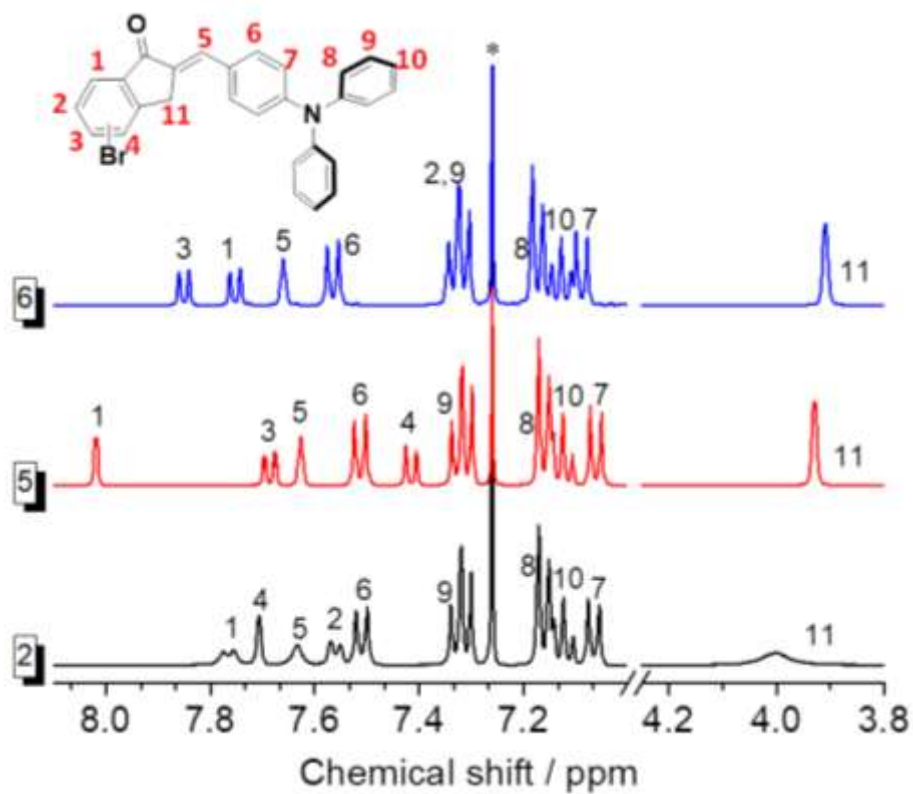


Figure S2. A comparison of the chemical shifts of ¹H NMR spectra for the bromo-substituted compounds **2** and **5–6** in CDCl₃ (500 MHz).

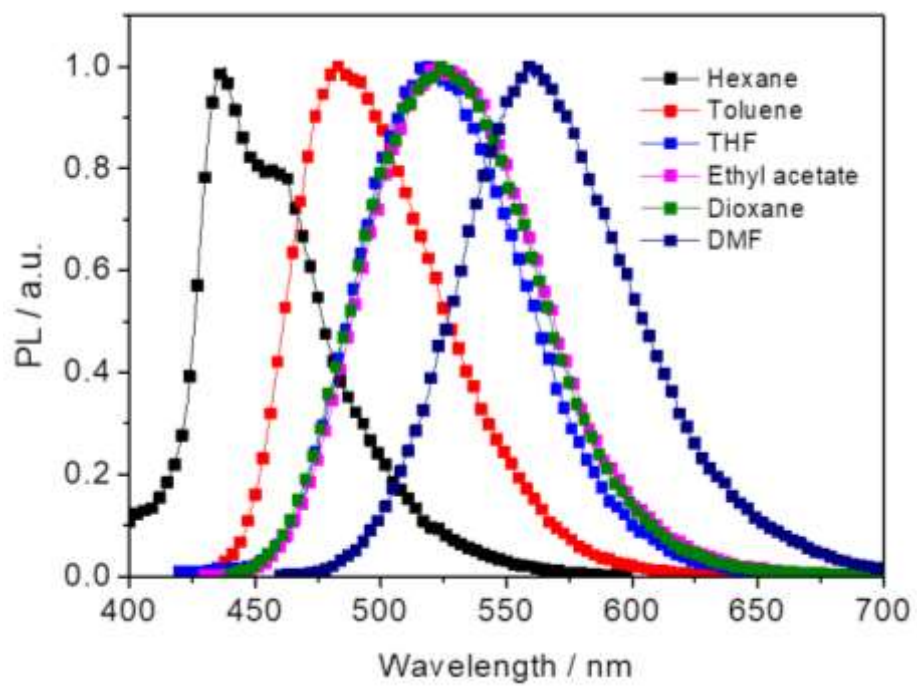


Figure S3. PL spectra of compound **1** in various solvents with different polarities.

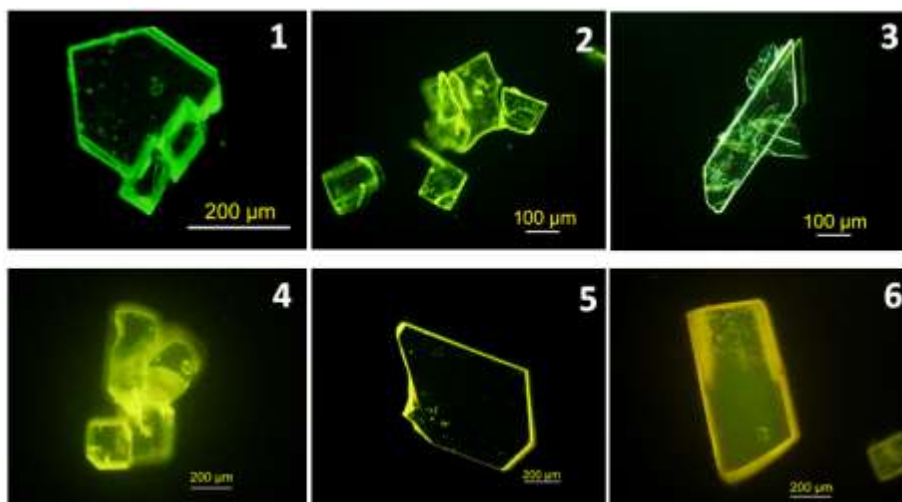


Figure S4. Microscopy images for crystals 1–6.



Figure S5. The schematic diagram of the jumping behavior of crystal 2.

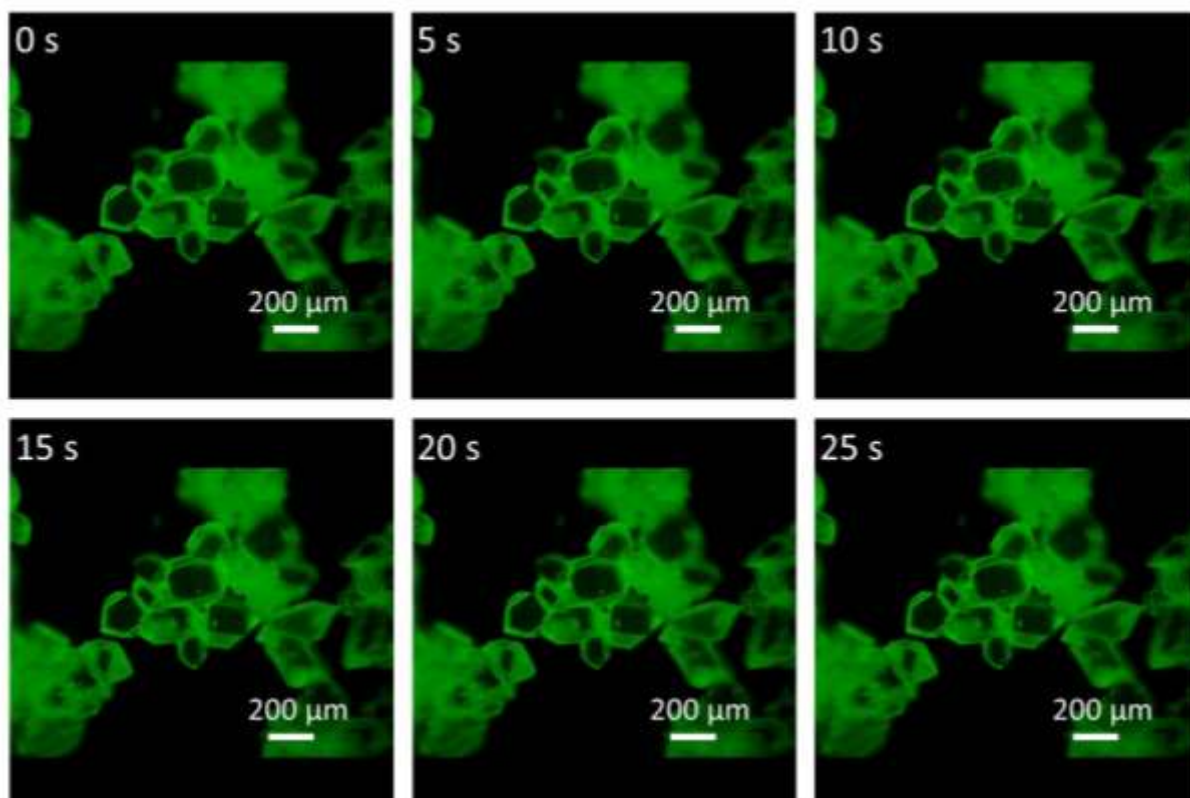


Figure S6. Microscopic images of crystal 1 at different times under UV irradiation (365 nm).

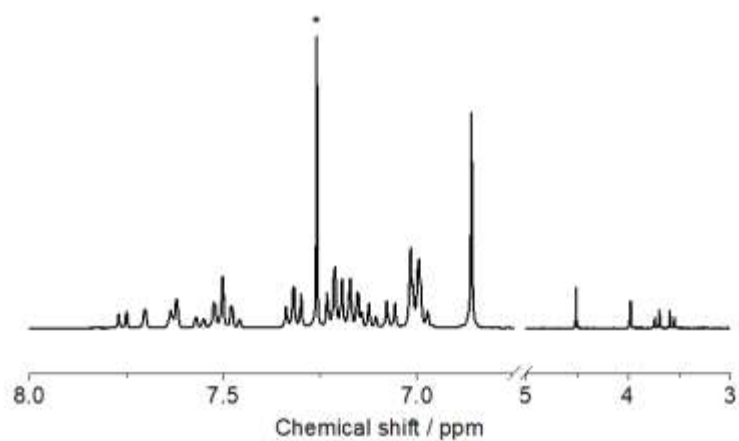


Figure S7. ^1H NMR spectrum (in CDCl_3 , 400 MHz) of purified X, which still shows two sets of signals .

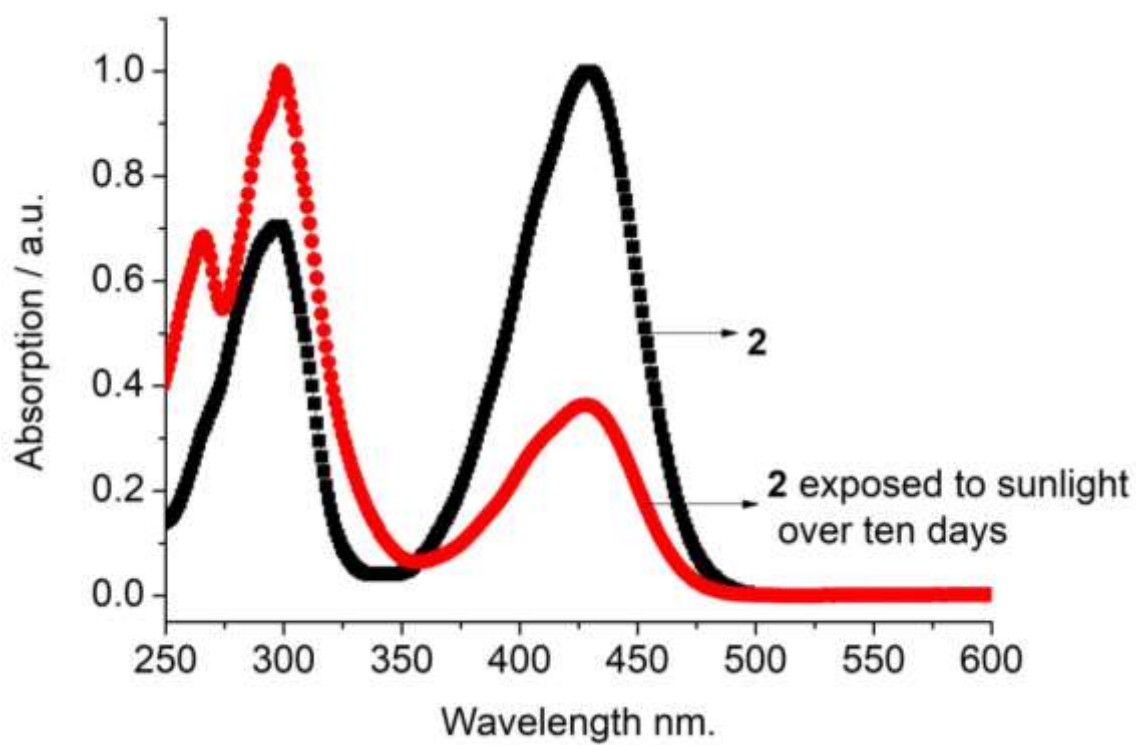


Figure S8. Absorption spectra in THF of crystal 2 before and after long-time sun exposure.

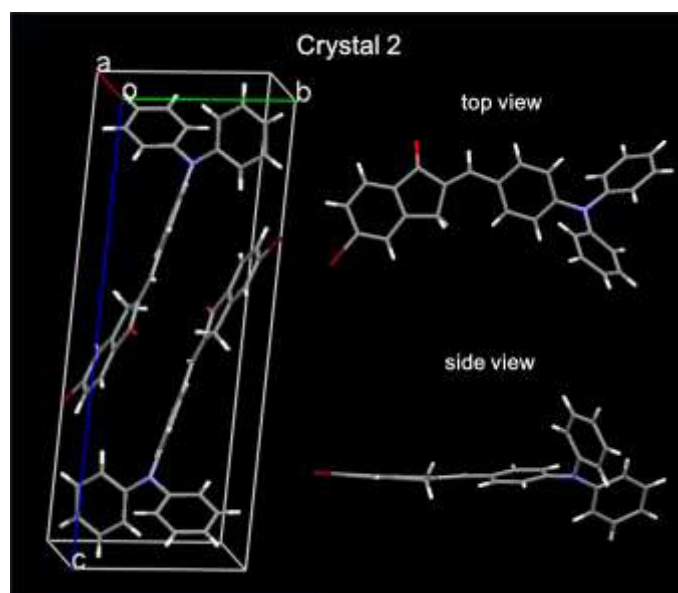


Figure S9. Unit cell for crystal 2.

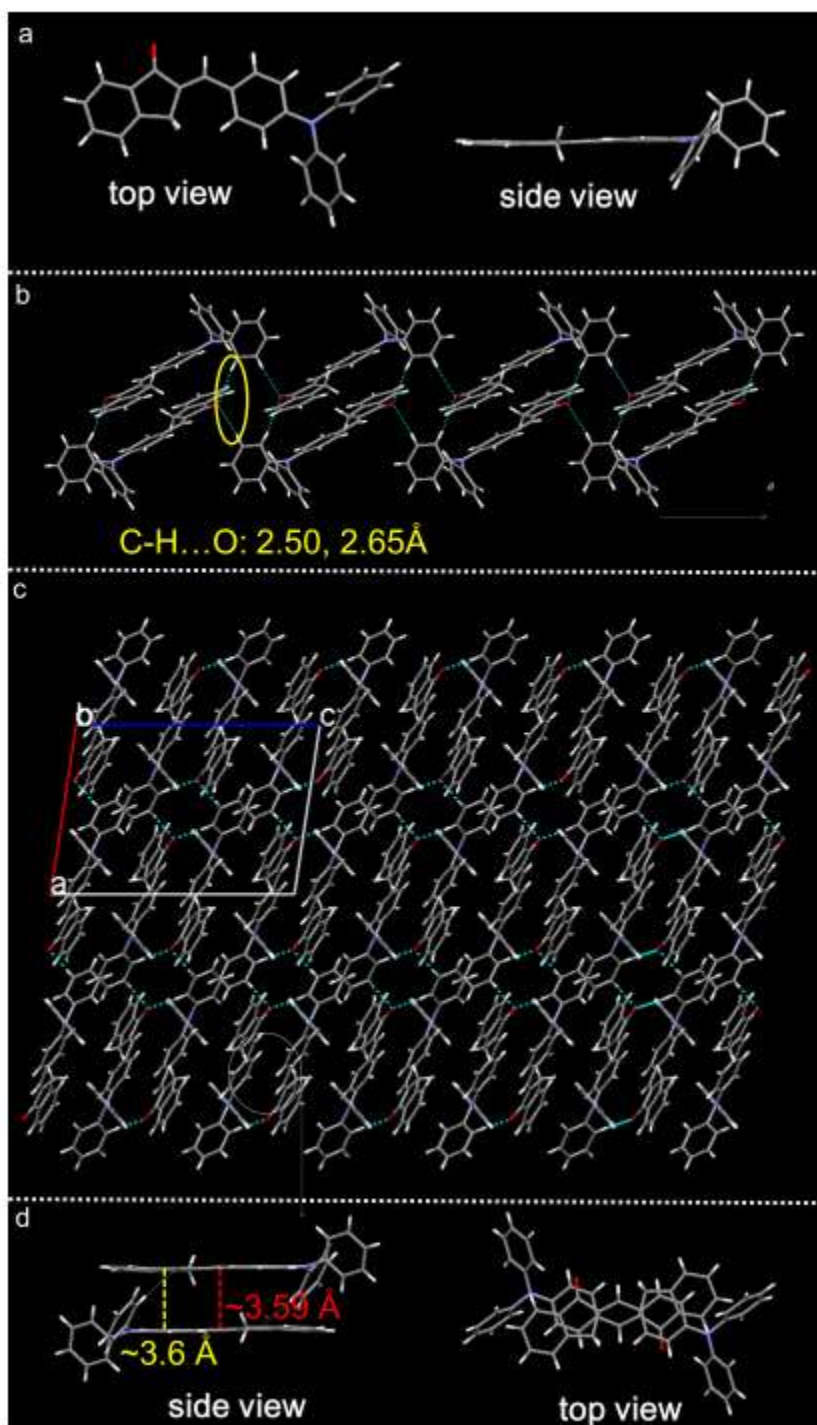


Figure S10. Crystal structure for compound **1**. (a) Top view and side view of molecular conformation in crystal **1**; (b) Molecular packing mode and weak intermolecular interactions along crystallographic *a* direction in crystal **1**; (c) Molecular packing structures in crystal **1**; (d) Side view and top view of the “molecular pair” structure with distances in crystal **1**.

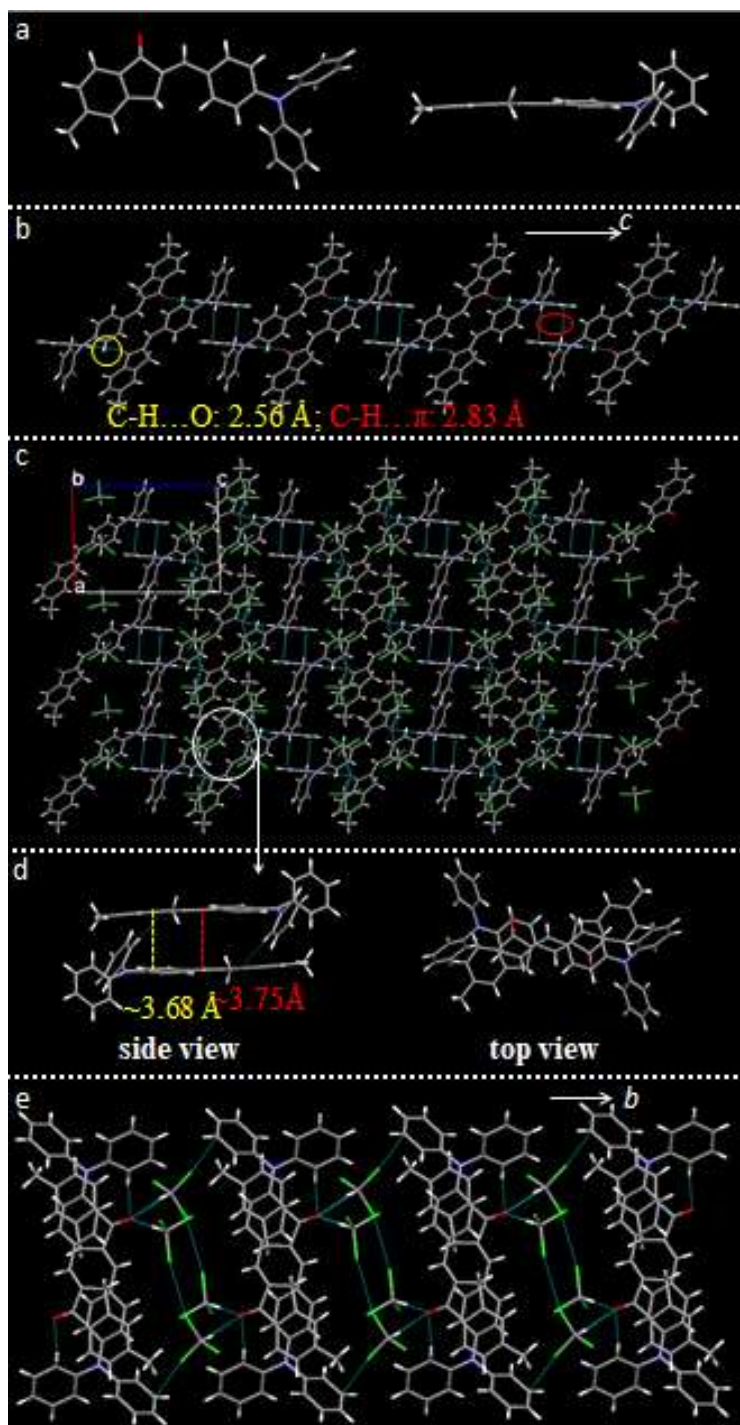


Figure S11. Crystal structures for compound 4. a) Top view and side view of molecular conformations; b) Molecular packing modes and weak intermolecular interactions along crystallographic *c* direction; c) Molecular packing structures at (010) crystal plane; d) Side view and top view of the “molecular pair” structure; e) CHCl₃ molecules participate the packing structure inside the crystal along *b* direction.

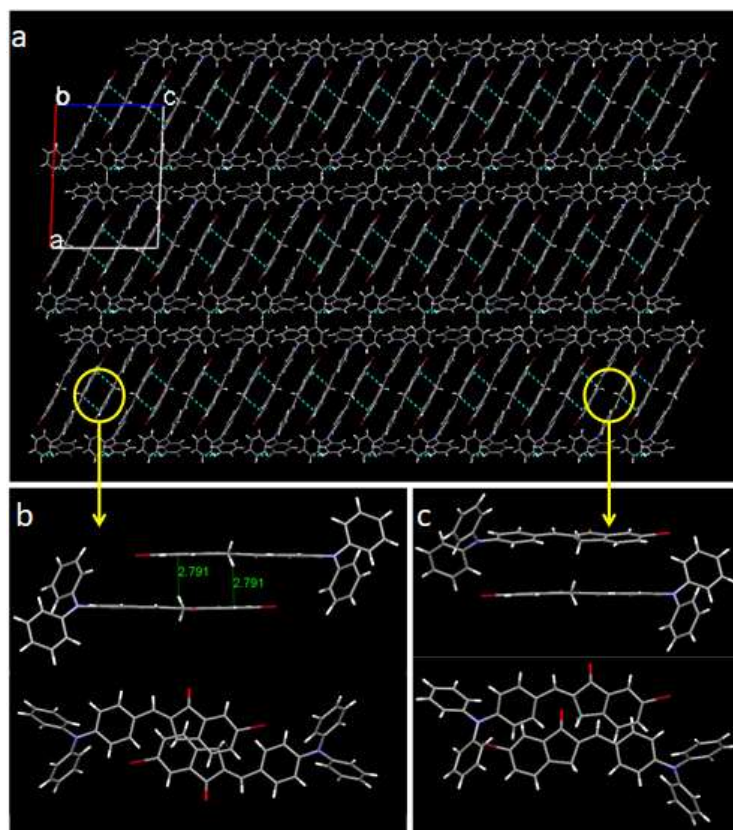


Figure S12. Crystal structures for compound **5**. a) Similar layered packing mode at (010) crystal plane as crystal **2**; b) Side view and top view of the non-typical “molecular pair” structure in **5** where molecules are dislocated with each other, different with the tightly face-to-face stacked “molecular pair” structure in crystal **2**; c) The dislocated adjacent molecules with no interactions in **5**.

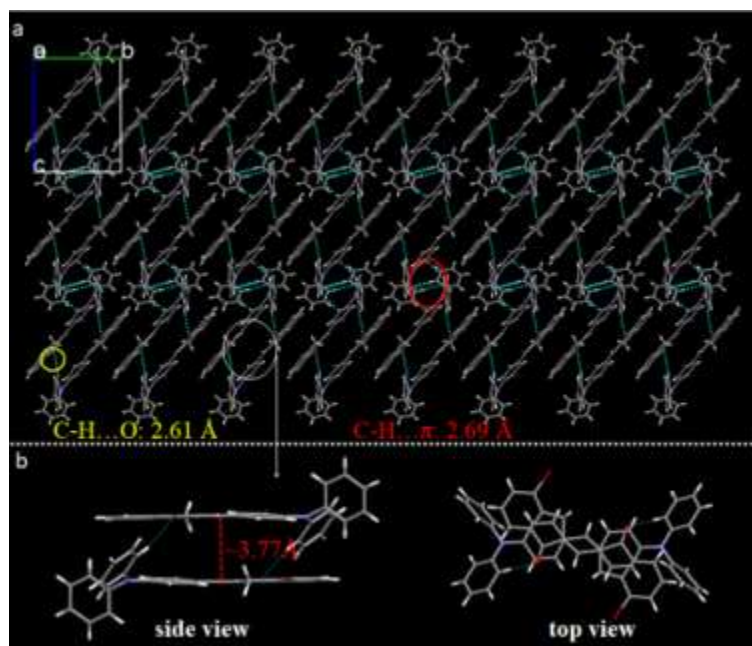


Figure S13. Crystal structures for compound **6**. a) Molecular packing structure at (100) crystal plane; b) Side view and top view of the “molecular pair” structure.

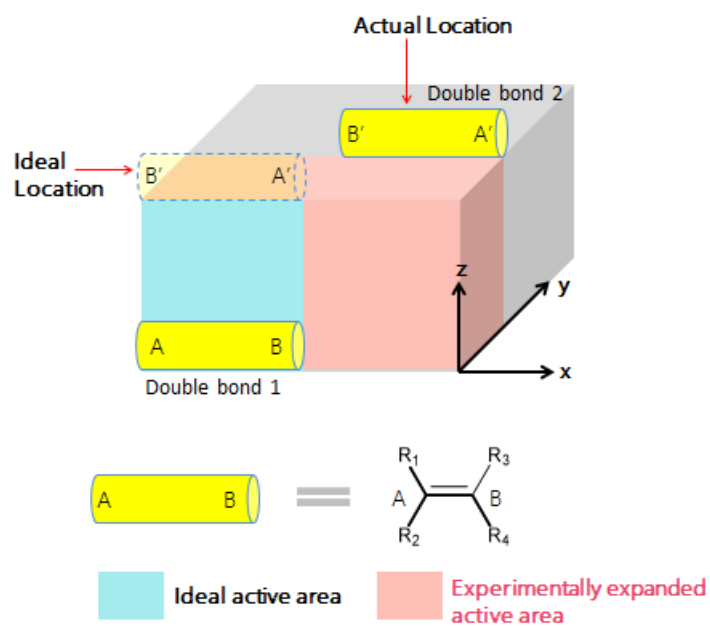


Figure S14. A 3D model diagram depicting the relative location of two double bonds in one “molecular pair“ in crystal 2. There exist some dislocations in both x and y directions.

Table S1. Various degrees of the dislocation for the two double bonds in different crystals.

Crystals	Offset distance in X / Å	Offset distance in Y / Å
1	0.63	1.60
2	1.08	0.82
4	1.17	1.04
6	0.92	1.17

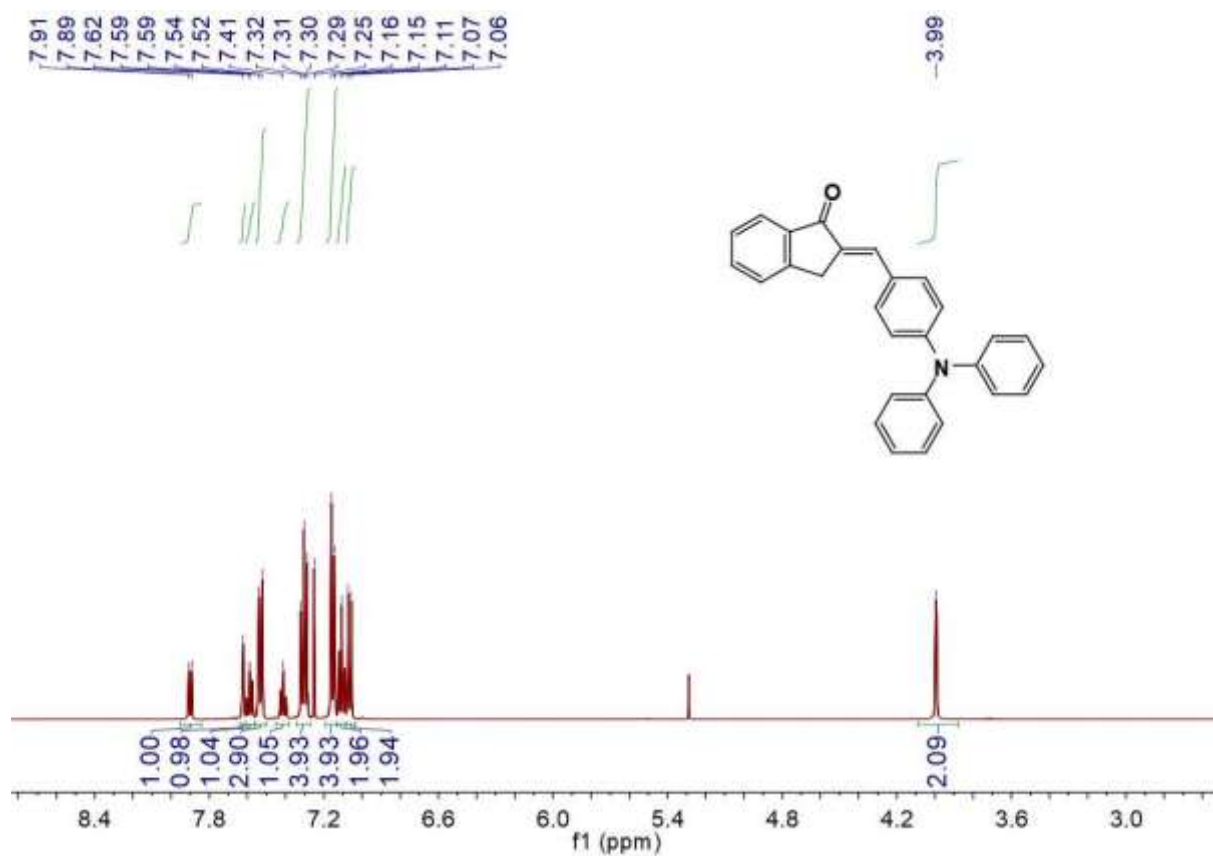


Figure S15. ^1H NMR spectrum (in CDCl_3 , 500 MHz) of crystal 1 under UV irradiation over 72 h.

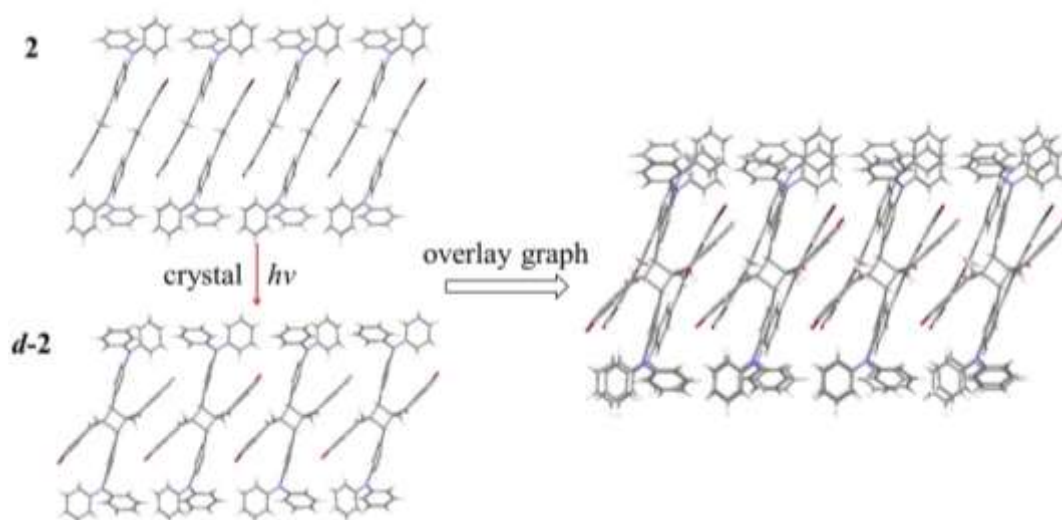


Figure S16. The overlay graph of the packing structures for crystal **2** and its cycloaddition reaction resultant **d-2**.

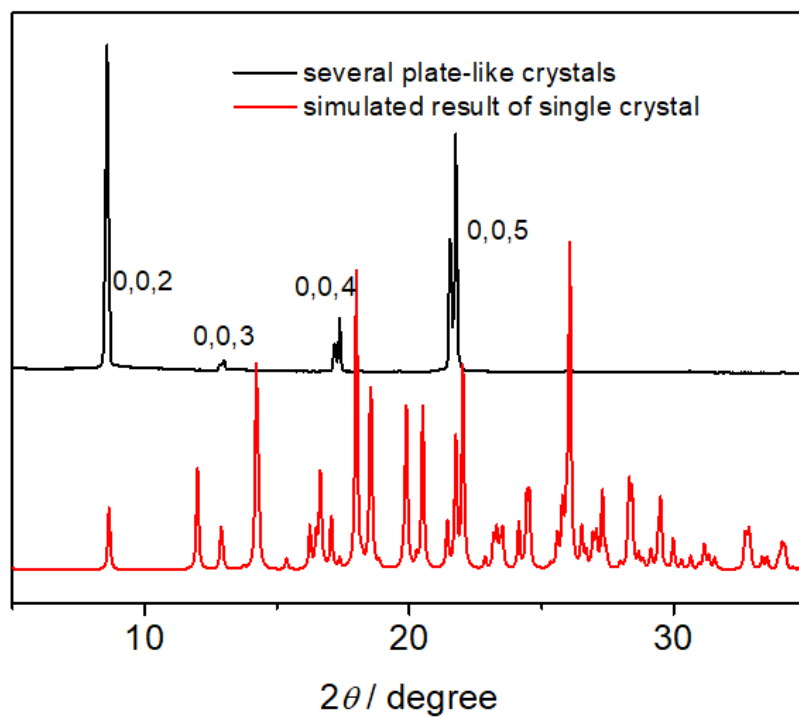


Figure S17. PXRD pattern for crystal 2.

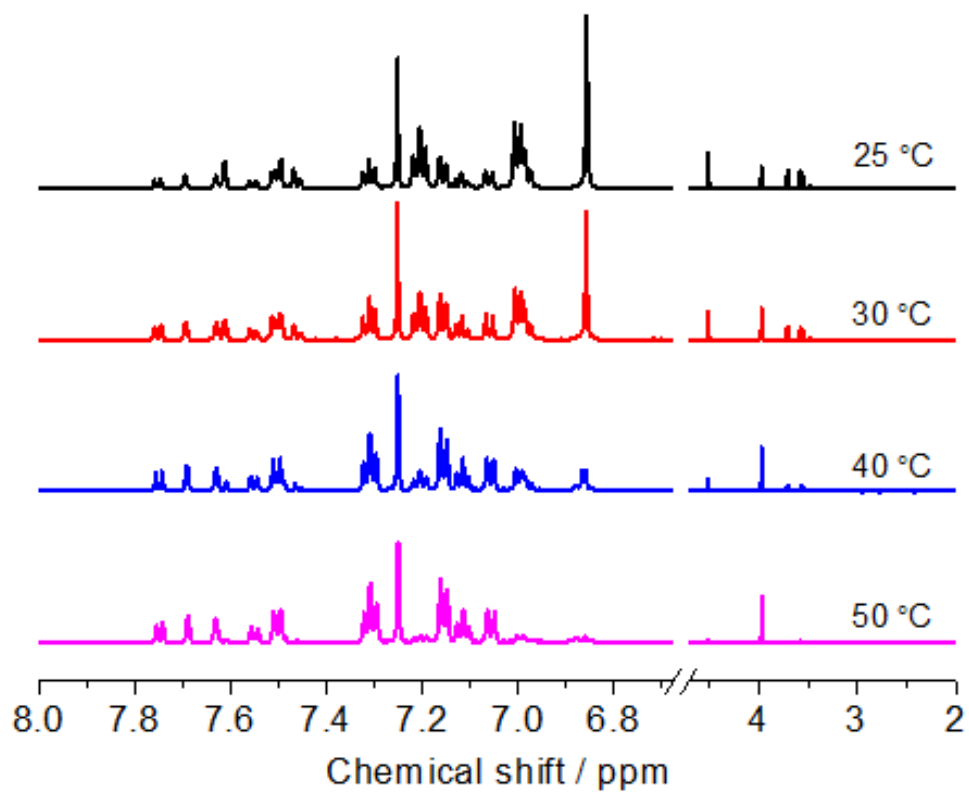


Figure S18. NMR spectra for the transformation of *d-2* to **2** over rising temperature in CDCl₃ (600 MHz).

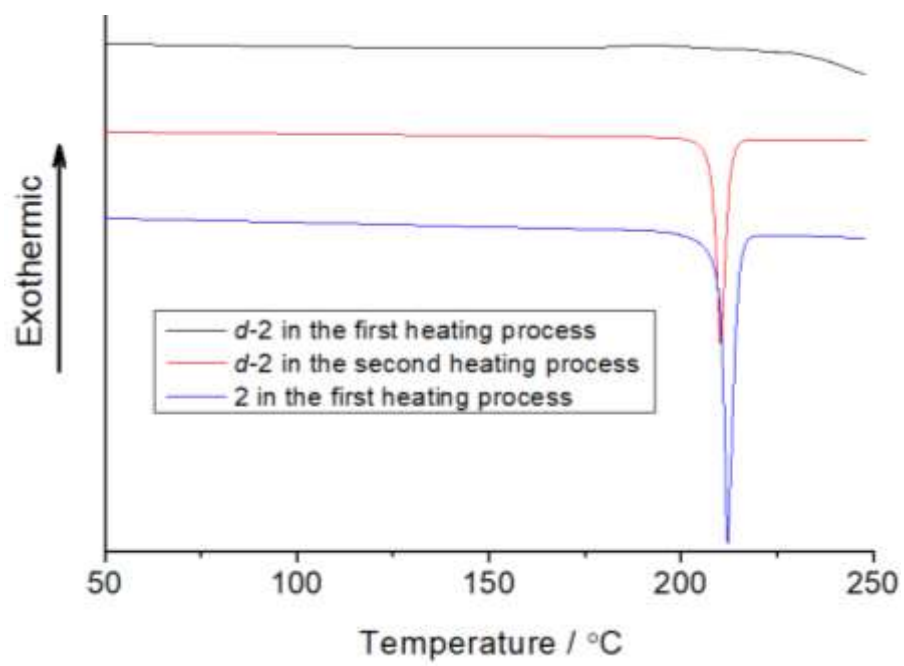


Figure S19. DSC curves of *d-2* and **2**.

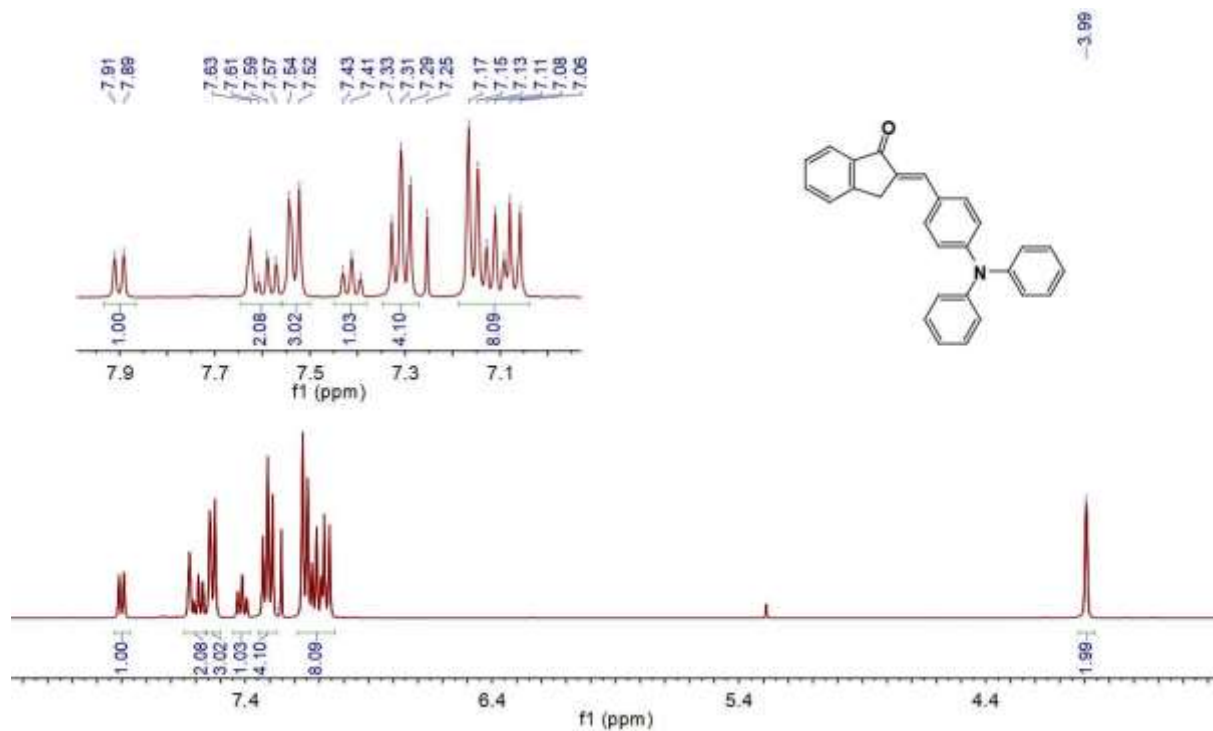


Figure S20. ^1H spectrum of compound **1** (400 MHz, CDCl_3).

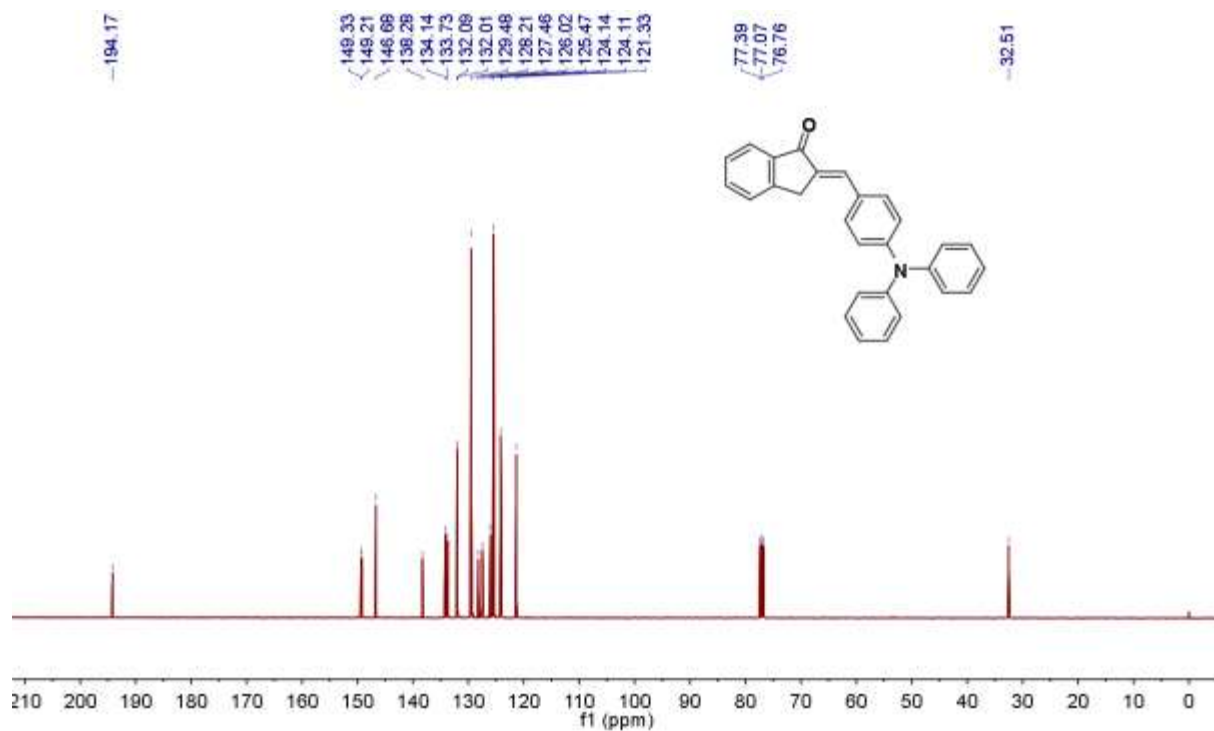


Figure S21. ^{13}C spectrum of compound **1** (100 MHz, CDCl_3).

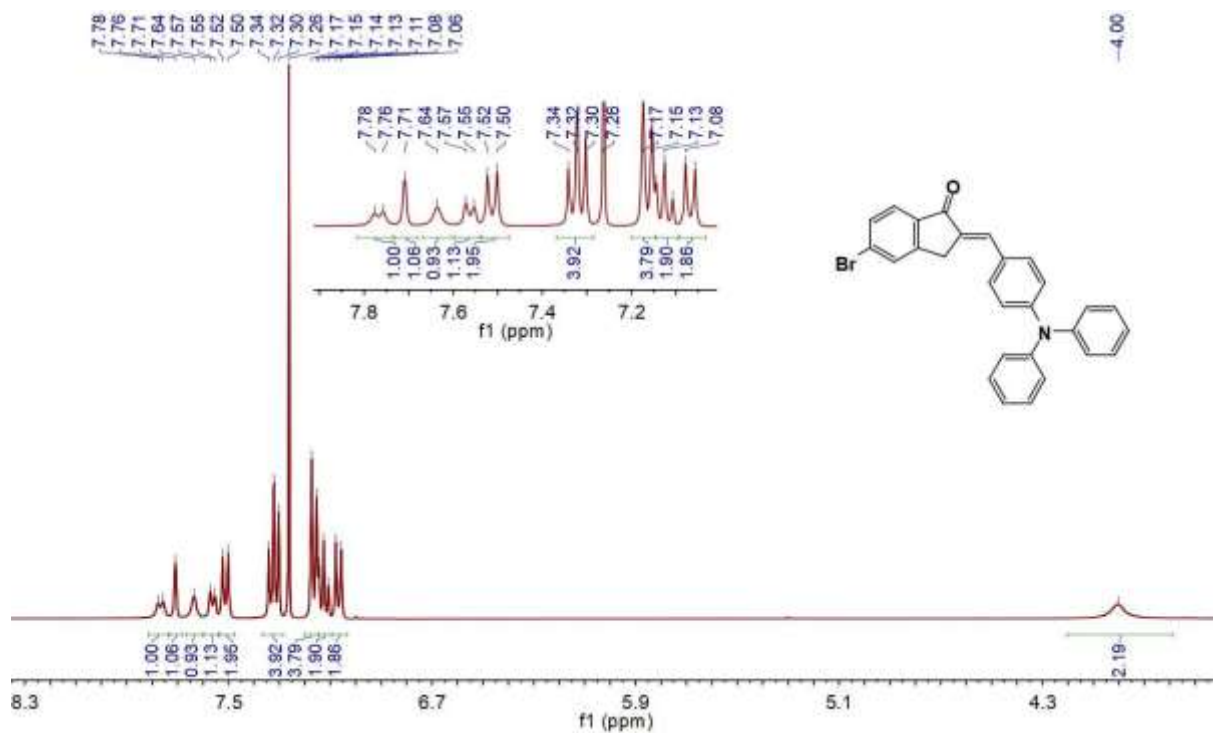


Figure S22. ¹H spectrum of compound **2** (400 MHz, CDCl₃).

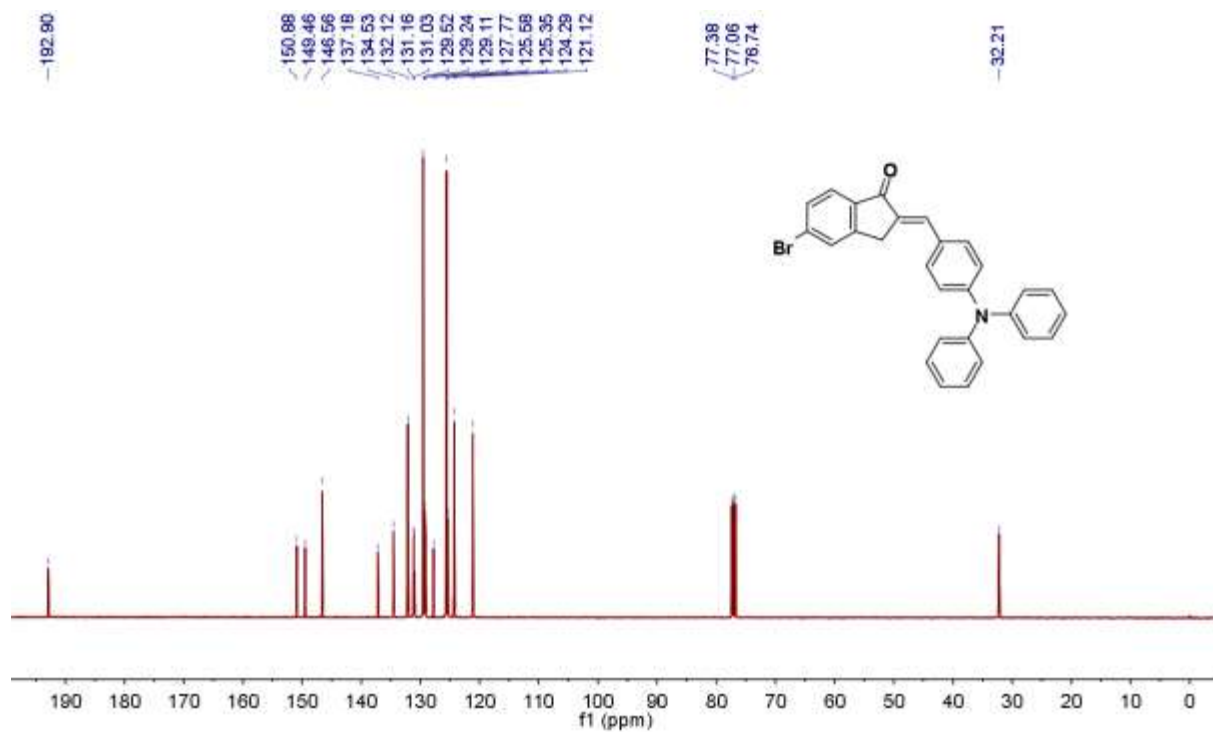
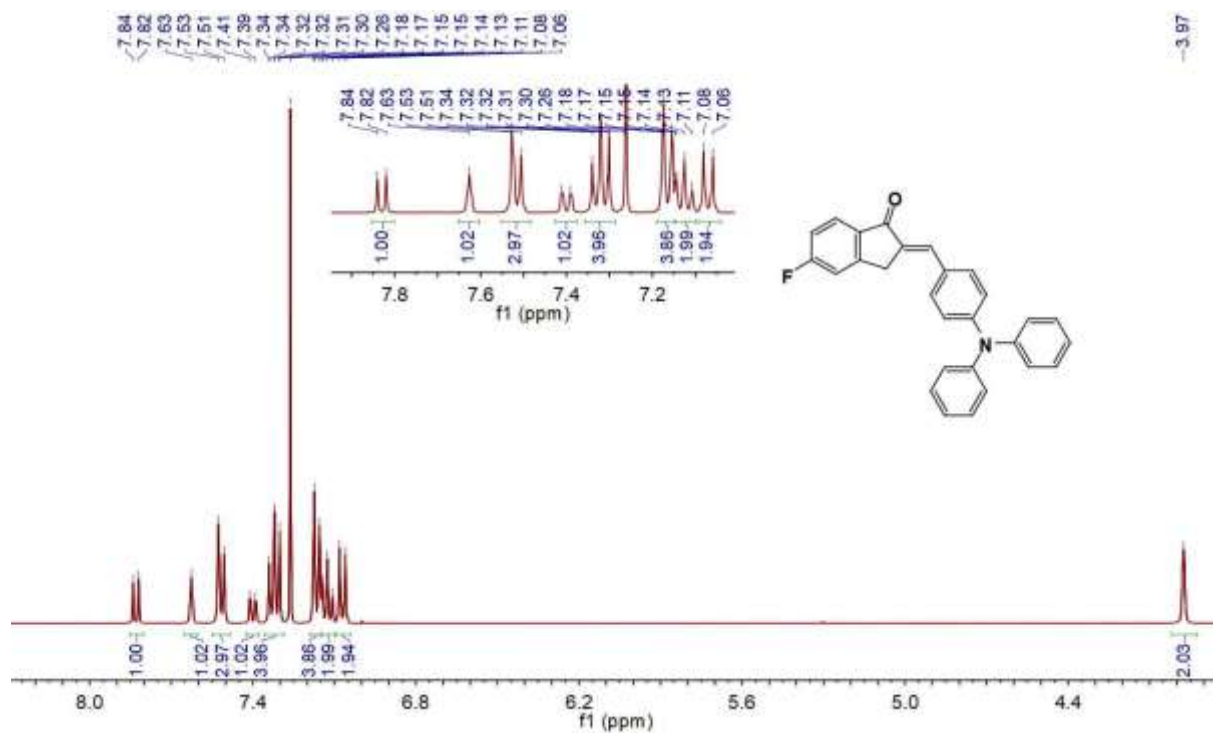


Figure S23. ^{13}C spectrum of compound 2 (100 MHz, CDCl_3).



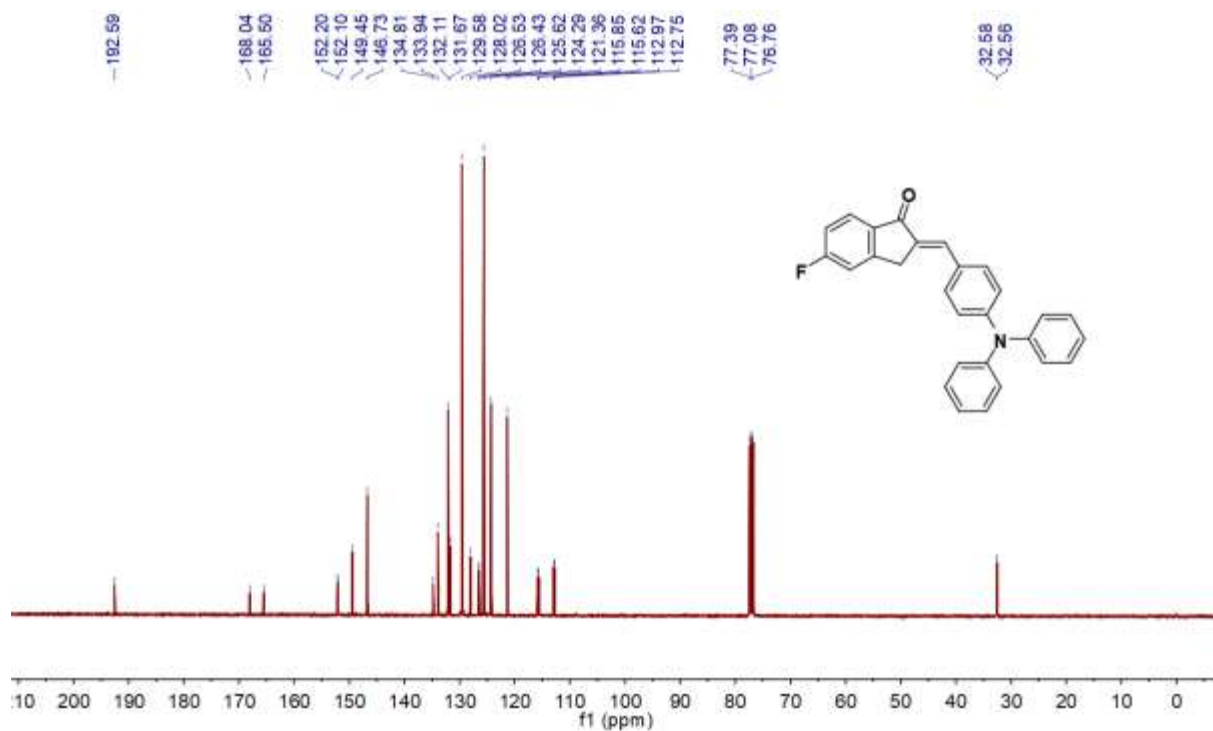


Figure S25. ^{13}C spectrum of compound **3** (100 MHz, CDCl_3).

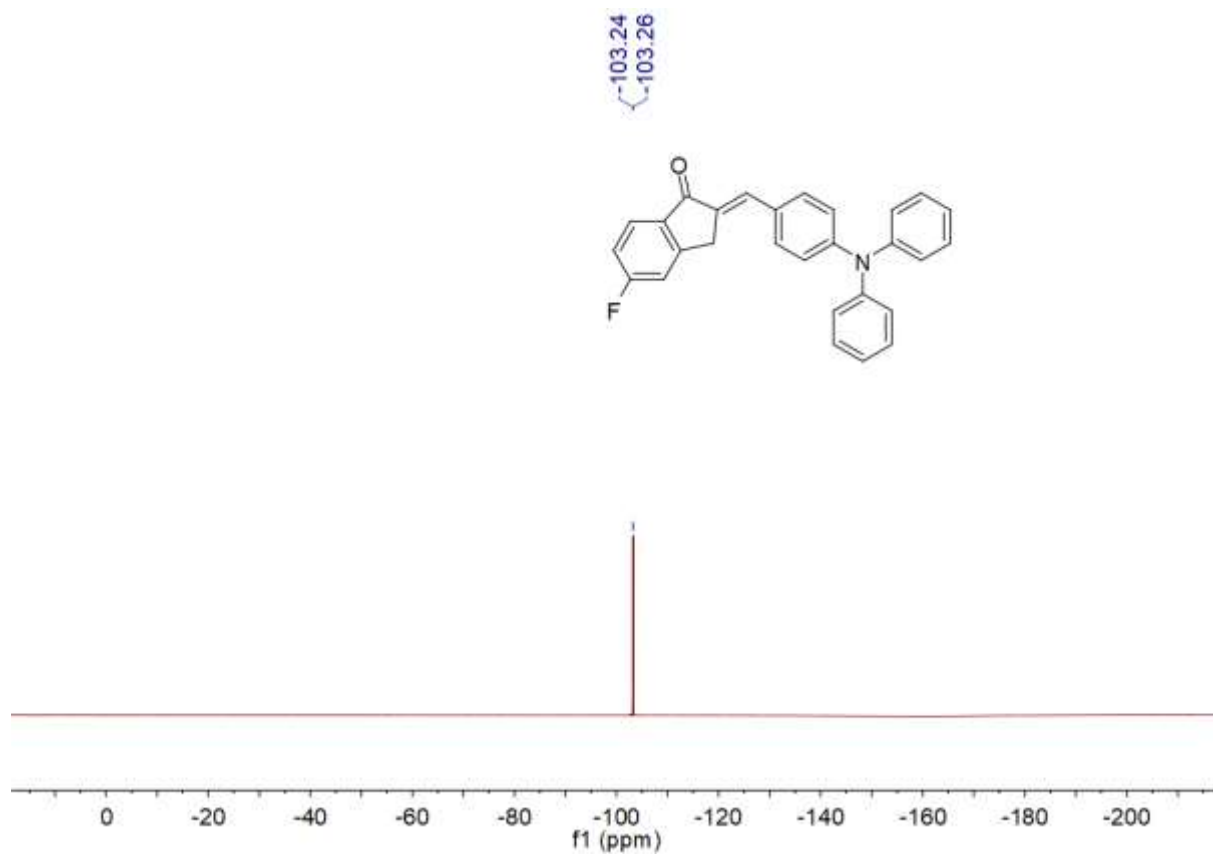


Figure S26. ^{19}F spectrum of compound **3** (376 MHz, CDCl_3).

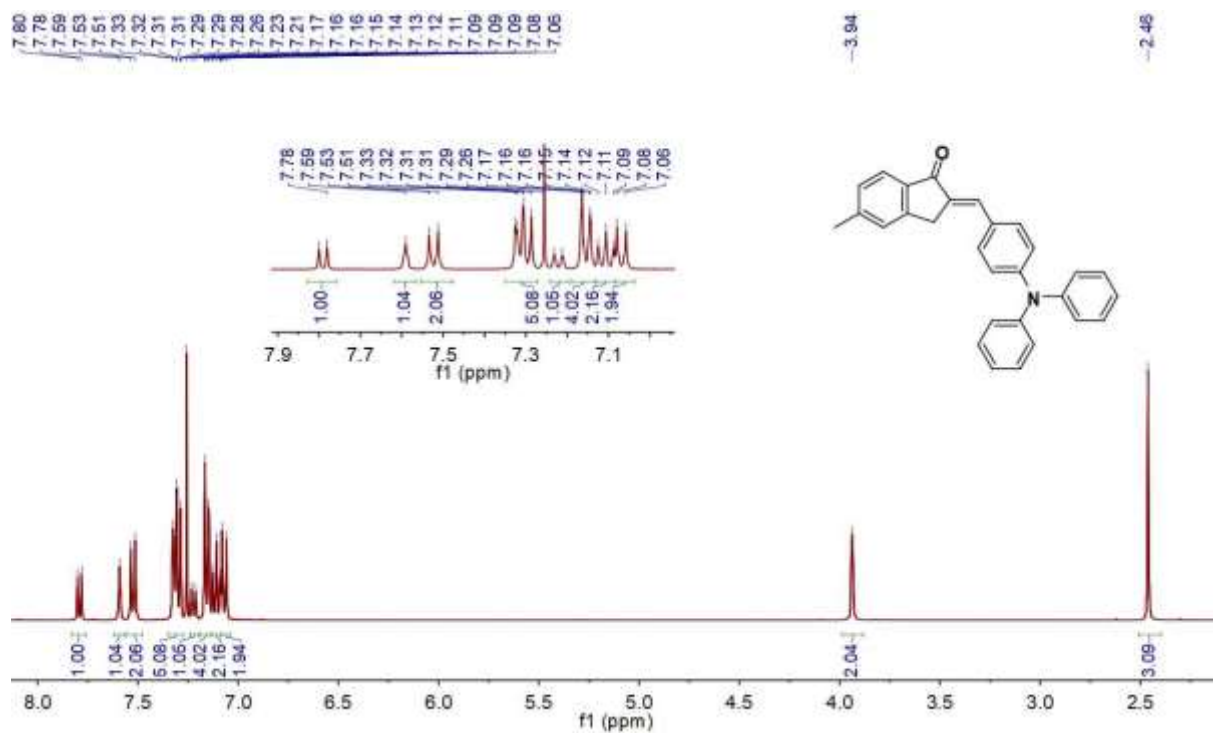


Figure S27. ^1H spectrum of compound 4 (400 MHz, CDCl_3).

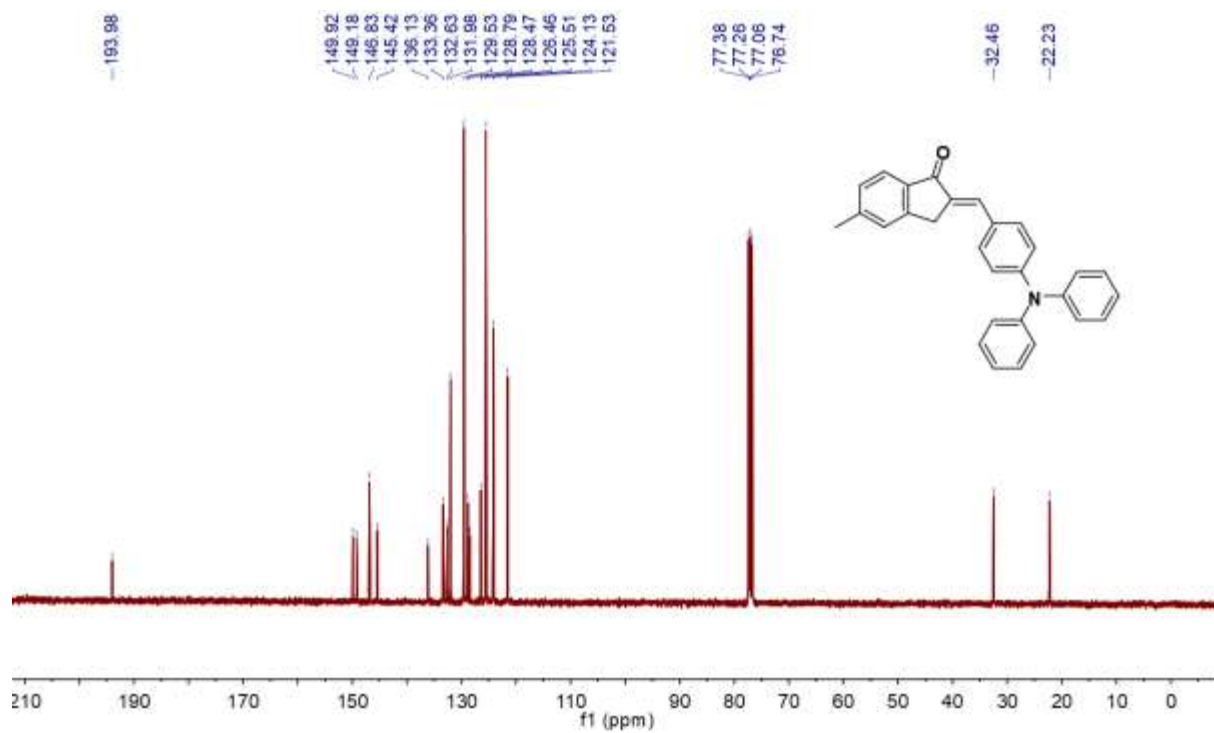


Figure S28. ^{13}C spectrum of compound 4 (100 MHz, CDCl_3).

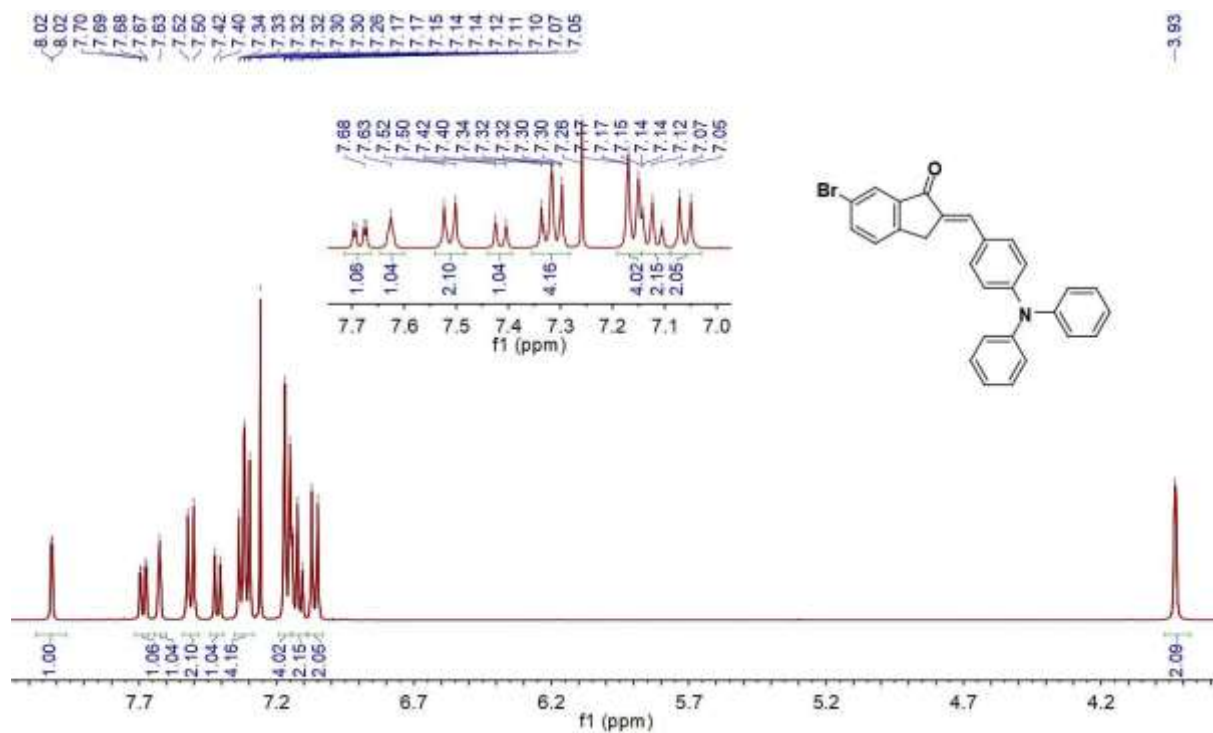


Figure S29. ^1H spectrum of compound 5 (400 MHz, CDCl_3).

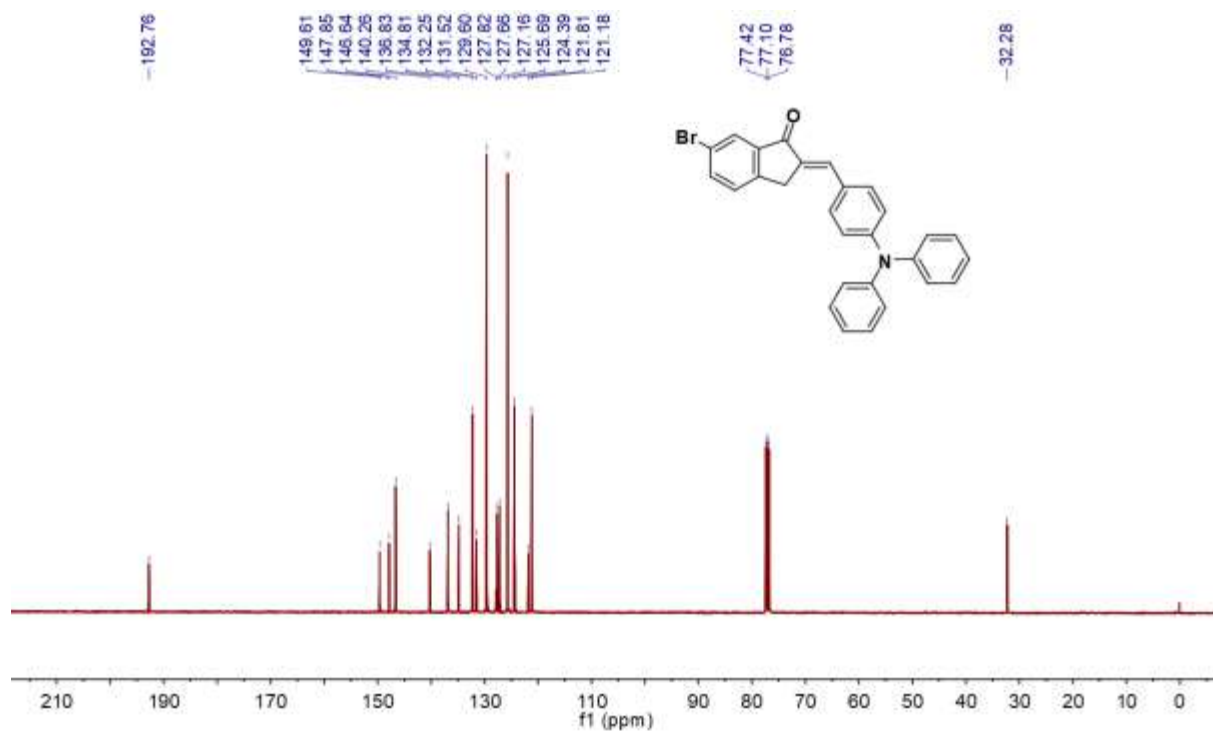


Figure S30. ^{13}C spectrum of compound **5** (100 MHz, CDCl_3).

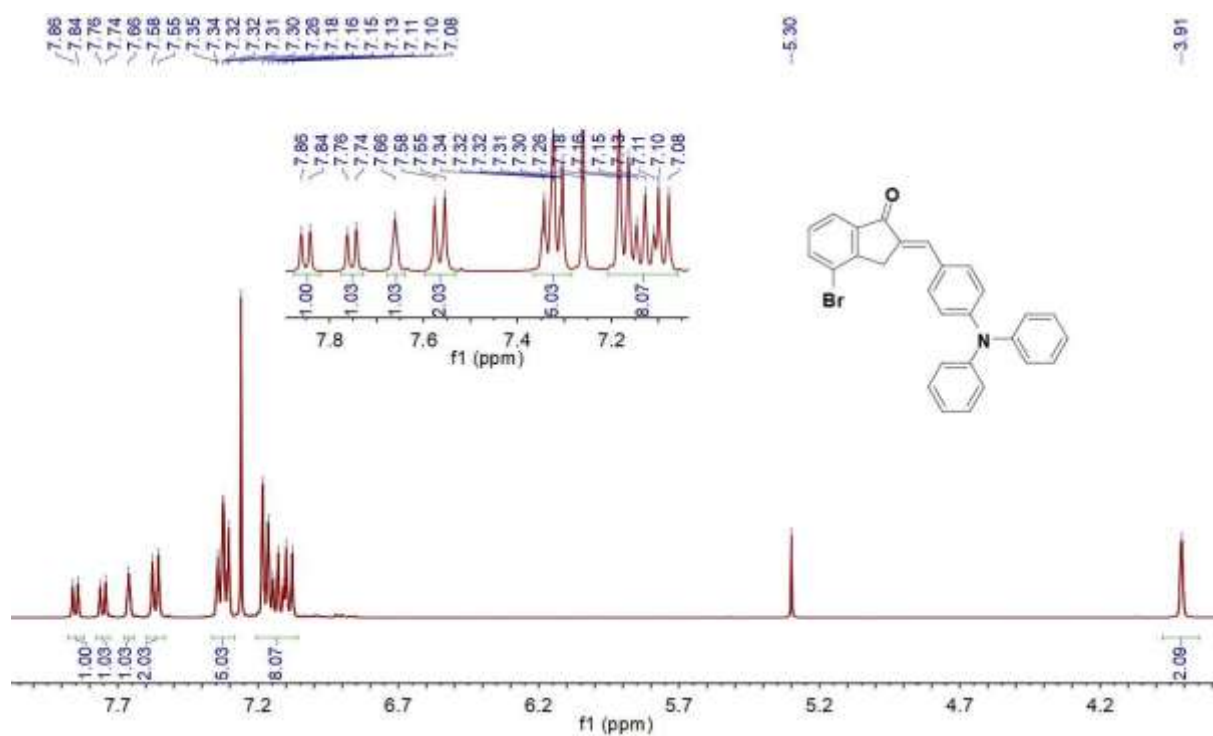


Figure S31. ¹H spectrum of compound **6** (400 MHz, CDCl₃).

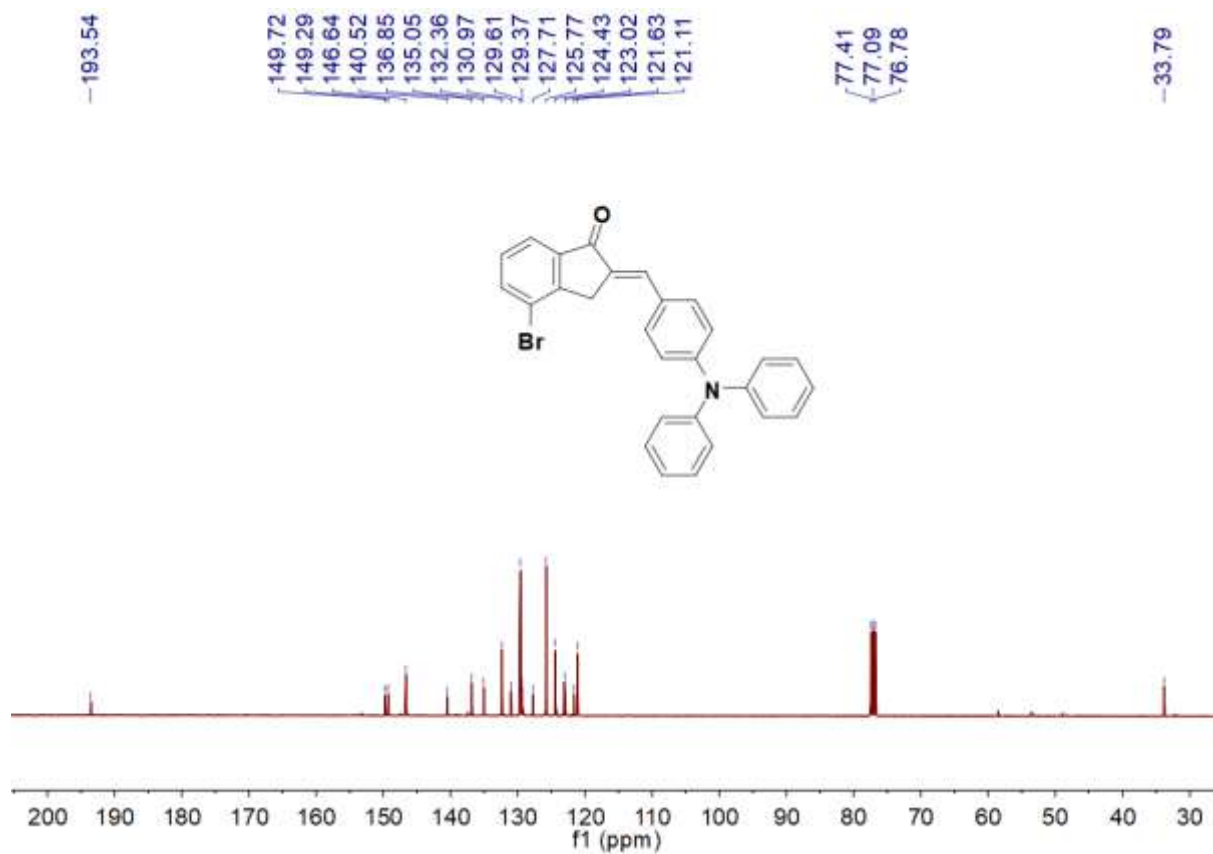


Figure S32. ^{13}C spectrum of compound **6** (100 MHz, CDCl_3).